On the use of X-ray computed tomography for the improvement of metal laser powder bed fusion process monitoring

Nicolò Bonato[1], Filippo Zanini[1], Simone Carmignato[1]

[1]University of Padova, Stradella San Nicola 3, Vicenza, Italy, e-mail: nicolo.bonato@phd.unipd.it | filippo.zanini@unipd.it | simone.carmignato@unipd.it

Abstract

Laser-powder bed fusion (LPBF) is increasingly used as a successful metal additive manufacturing technology in different industrial sectors, such as biomedical and aerospace, especially for the production of parts with high geometrical complexity. However, LPBF is still affected by repeatability issues and the presence of several defects within the fabricated components. This aspect is therefore a hindrance in the spreading of this prospective technology, which in several cases is still not able to meet the stringent quality requirements imposed by such industries. In order to overcome these issues, X-ray computed tomography (CT) acquires a fundamental role in the understanding of critical aspects and for process development and optimization. Also considering the growing interest regarding the development of LPBF process monitoring systems, which seek to identify and possibly correct defects during fabrication, CT is very much needed for the generation of reference data concerning actual geometry and internal defects. Nevertheless, this implies the need for an accurate comparison between datasets obtained by in-process acquisitions and post-process measurements, with the aim of successfully correlating process events to actual defects. However, to enhance the comparison accuracy, deformations occurring during and after manufacturing need to be considered when performing in- and post-process data registration, given that this aspect is greatly affecting the outcome of correlations.

This work studies a sample geometry that is specifically developed for enhancing data registration accuracy, along with the related alignment procedure. The methodology has also the advantage to be applicable to any kind of in-process monitoring data, despite this paper uses optical imaging for the acquisition of long-exposure digital images, which proved to be suited for detecting spatter particles. Post-process datasets were obtained through metrological X-ray computed tomography, which provides detailed information regarding internal defects.

Keywords: X-ray computed tomography, additive manufacturing, dimensional metrology, in-process monitoring

1 Introduction

Additive manufacturing (AM) is attracting increasing interest from both industrial and research fields due to several benefits, among which the great sustainability resulting from the efficient material consumption and the chance of fabricating parts with a very complex geometry [1]. Additionally, the intrinsic flexibility of AM enables a quicker industrial reconversion, enhancing companies' resilience to market fluctuations or other unforeseen events [2].

This experimental work is specifically focused on metal laser powder bed fusion (LPBF), an additive manufacturing technology where the feedstock material is in the form of metal powder, which is spread into thin subsequent layers starting from a building platform. The generated powder bed is selectively melted at specific locations by the energy of a focused laser beam. The heat is quickly dissipated towards the building platform through the support structures, which have also the function of anchoring the part to the platform itself to prevent possible deformations. Once a layer of material is consolidated, the above-mentioned steps repeat iteratively layer by layer, until the part is completed.

LPBF of metals is often chosen for manufacturing functional components for aerospace and automotive applications that need to satisfy challenging requirements in terms of strength-to-weight ratio, as well as for fabricating parts with controlled lattice architectures and surface texture, e.g., in the biomedical field [3]. In these contexts, assuring the quality and the repeatability of parts built by LPBF is essential for meeting the stringent certification criteria imposed by high-added value industries.

However, the process is still affected by a lack of stability and robustness, which need to be overcome for widening the adoption of LPBF across different industrial fields [4, 5]. To this aim, significant research efforts are dedicated to increase the understanding of LPBF process dynamics leading to defects, and to improve the process itself and the obtained products by reducing such defects. In particular, in-process LPBF monitoring is seen as a fundamental contribution to the cause. Indeed, observing and measuring process events, often referred to as process signatures [6], paves the way to correct potential defects in real-time by acting on the process itself under a closed-loop control [7]. In this field, literature shows works related to the observation of various process signatures, as classified in [8]. Although co-axial monitoring systems using photodiodes and/or high-speed cameras are capable of gathering data which are very close to process dynamics (e.g., melt pool monitoring) [9, 10], off-axal setups are often preferred in industry due to the lower costs and easier implementation [11-13]. The latter, in fact, consists in the installation of sensors including high-resolution cameras in the visible or in the near-infrared/infrared range, which allows capturing images of either the entire powder bed or consolidated material layer, lowering the amount of data to handle with respect to co-axial acquisitions [14]. In order to efficiently use the in-process gathered data, an important aspect to be

https://doi.org/10.58286/27706

considered is the correlation between anomalies observed during the process and actual defects occurring due to such anomalies. In this context, X-ray computed tomography (CT) is often used to study this correlation, thanks to its capability of providing comprehensive information concerning internal defects as well as dimensional and geometrical deviations in both accessible and difficult-to-access regions of the fabricated parts [15]. CT non-destructive measurements are hence treated as ground truth for porosities and deformation that can be critical for mechanical properties and for the fatigue behaviour in components subjected to cyclic loads [16]. What emerges from previous works focused on establishing a correlation between process signatures registered during LPBF fabrication and defects measured by CT after the samples have been detached from the building platform, is that determining clear correlations is not trivial and not possible in most cases [17]. Two possible explanations are: (i) some anomalous process conditions can lead to defects on the observed layer that are partially or completely "cured" when producing the subsequent layers, considering that the laser parameters are typically set to promote intra-layer bonding by re-melting also the previous layers; (ii) after-build deformations can modify the relative position/orientation of consolidated layers with respect to the original generation and monitoring position.
The second aspect is addressed in this work by considering that the comparison of in-process and post-process datasets must rely on an accurate data registration that takes into account possible after-build deformations. With an accurate data alignment also the first aspect can be better studied, by reliably distinguishing relevant and not relevant process anomalies. In order to improve the accuracy of alignment between in-process and post-process gathered data, adequate sample design and alignment procedures are needed, as remarked in [18]. However, research works published so far investigated the correlation using simple geometries, such as cylinders or cubes, with no use of fiducials properly designed for aiding the alignment [19].
Figure 1 shows a comprehensive LPBF process-monitoring workflow, including sample design, in-process monitoring and post-process CT analysis. This work studies a new sample geometry, firstly introduced in [20], with specifically designed reference fiducial, following the manufacturing- and metrology-related design guidelines reported in the box to the right of Figure 1 and discussed in Section 2.1. An alignment procedure is also discussed.
The proposed method is then verified using actual LPBF parts and applied to a real case study where in-process monitoring has been performed through an off-axis long-exposure digital imaging.

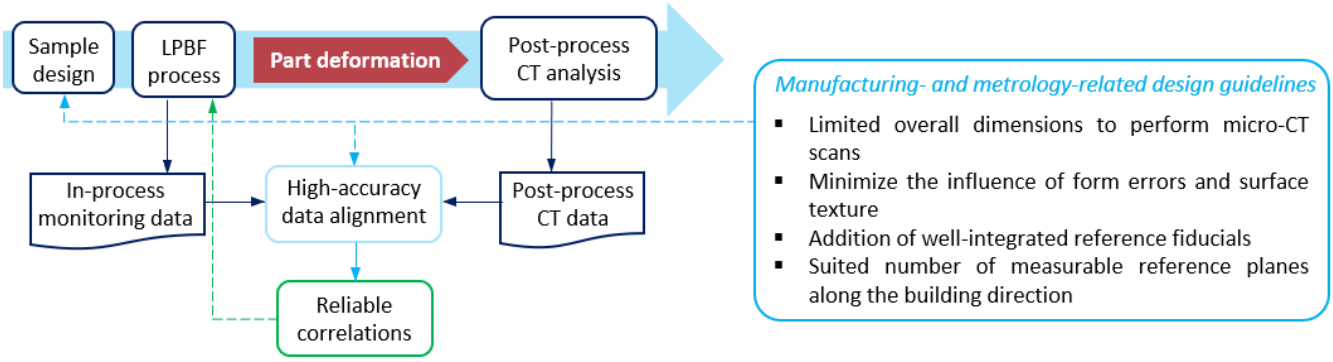

Figure 1 – Schematic representation of LPBF process workflow with the integration of design guidelines for high-accuracy data alignment

2 Material and methods

Section 2.1 describes the sample geometry and the procedure proposed to improve the alignment between in-process monitoring data and post-process CT measurements. Furthermore, samples production conducted by LPBF process is also addressed. Post-process CT measurements are then introduced in Section 2.2, in the context of providing ground truth information with respect to internal porosities.

2.1 Sample design and manufacturing

In order to improve the accuracy of the comparison between in-process monitoring and post-process CT scans, the sample geometry must be designed with adequate reference fiducials to be used for registering data acquired in different moments (i.e., during and after fabrication). Design requirements should depend on the LPBF process, while others are metrology-related. As shown in the box to the right of Figure 1, these manufacturing- and metrology-related design guidelines can be resumed into four main points:

1. The overall dimension of the sample has to guarantee the capability of performing high-resolution CT scans. The high resolution is needed to enable the detection and measurement of critical defects, whose dimensions are often in the order of few micrometres.
2. Form errors and surface texture should be minimized as they could affect fitting operations and measurements done on the CT reconstructed reference fiducials. Indeed, the typical surface texture of LPBF is highly complex and depends on different factors, but in principle it can be made more homogeneous by properly orienting the fiducials' surfaces with respect to the building direction.

3. The fiducials need to be well-integrated in the global sample geometry, in order to be representative of actual part deformation and not to be affected by local deviations. In addition, too small features should be avoided as they may not be rigid enough to sustain local stresses without drifting from their nominal.
4. With the purpose of considering both in-plane and out-of-plane deviations when aligning in-process and post-process data, several reference planes should be measurable along the building direction.

Based on these requirements, the geometry illustrated in Figure 2 was designed. The global shape is a cylinder built on a flat base (A in Figure 2), whose normal was chosen as a reference for the building direction (z-axis). Starting from this shape, specific reference fiducials were integrated. These features are constituted by an internal pocket with a horizontal plane (P), on top of which a cylinder (C) is built with side connection to the main shape (beneficial for avoiding localized deformations through enhanced heat dissipation during the fabrication). The sample integrates a total of 21 fiducials, arranged in seven different levels along the building direction. Each level features three equally spaced fiducials, i.e., disposed at 120 degrees with respect to each other. Both cylinders and planes are subjected to least-squares fitting and a point is retrieved from the intersection of the cylinder axis with the horizontal plane. A local plane can finally be generated from the three points obtained in each level. The measured coordinates of points and the position of the obtained planes provide useful information on local deviations and deformations of the fabricated sample. Finally, with the aim of breaking the symmetry of the base of the sample for an initial rough alignment, a notch was created.

The vertical walls of the built cylinders allow obtaining a more homogeneous surface texture with reduced roughness and staircase with respect to down-facing or tilted surfaces. Furthermore, the dimensions of the features were modelled to be sufficiently large if compared with the order of magnitude of surface imperfections typical of vertical walls.

In this work, parts with the proposed geometry were produced by using a Sisma MYSINT100 (Sisma SpA, Italy). As for the material, Ti6Al4V was chosen for its broad adoption in LPBF. With the aim of stimulating the occurrence of defects, the main process parameters such as laser power and speed were purposely modified with respect to the optimized set. Support structures anchoring the sample to the platform were also modelled to further stimulate geometrical and dimensional deviations. Finally, with the purpose of reducing the surface roughness of the horizontal planes, two subsequent re-melting steps were performed.

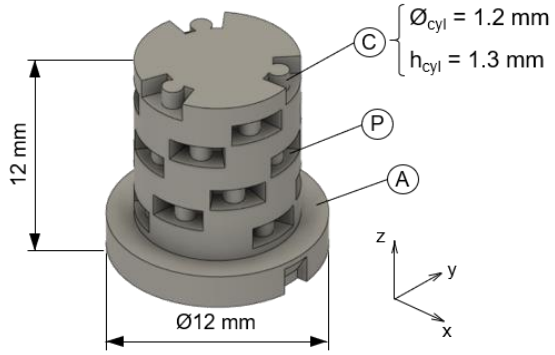

Figure 2 – Schematic representation of the proposed geometry

2.2 CT post-process analyses

The fabricated samples were scanned with a metrological CT system (Nikon Metrology MCT225), equipped with a micro-focus X-ray source, a 16-bit X-ray detector with a 2000×2000 pixel grid, high-precision guideways and controlled cabinet temperature (20 ± 0.5 °C).

Table 1 lists the scanning parameters for the specimens, resulting in a voxel size equal to 7.7 μm, which is adequate for porosity analysis [21]. A 0.1 *mm* copper physical filter was interposed between the X-ray source and the object in order to reduce beam hardening. Once the 2000 projections have been acquired, they were exploited for reconstructing the 3D volume of the scanned samples.

Table 1 – CT parameters

Parameter	Value
Voltage	200 kV
Current	35 µA
Power	7 W
Exposure time	1420 ms
Frames per projection	1
Nr. of projections	2000
Physical filter material	Cu
Physical filter thickness	0.1 mm
Voxel size	7.7 µm

The obtained volumes were then analysed by means of the software VGStudio MAX 3.2 (Volume Graphics GmbH), where a local-adaptive surface determination was performed.

3 Application and verification of the proposed alignment method

Once the surface has been determined as explained in Section 2.2 on the CT reconstructed model, the least-squares fitting of the geometrical elements (cylinders and planes) was carried out as discussed in Section 2.1. First of all, the reconstructed volume was roughly aligned to the CAD model by means of a best-fit registration. Upon the volume has been registered, a measurement template (created already aligned to the CAD volume) was imported and applied to the CT volume. The template contains all the features that need to be fitted for performing a more accurate alignment and the measurements of interest, i.e., all the horizontal planes (P in Figure 2) and the cylindrical vertical surfaces (C in Figure 2). Figure 3a shows the measurement template aligned to the CAD model. It is worth highlighting that the horizontal fitting surfaces, highlighted in green, were modelled with an inward offset of 0.15 mm for each side with respect to the CAD planes. This choice guarantees the fitting of representative planes by excluding critical regions such as borders, which are often more elevated than the inner horizontal geometries, and the nearby vertical walls surfaces. The cylindrical fitting surface was also reduced in its height from 1.3 mm to 0.75 mm, in order to avoid the influence of the horizontal plane at the bottom and of the dross formation phenomena at the top.

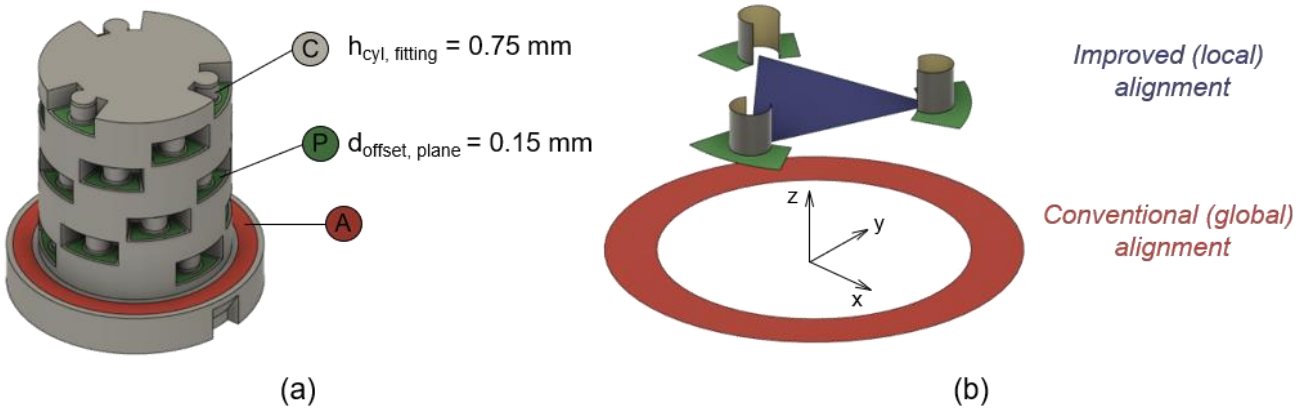

Figure 3 – Alignment of the measurement template onto the CAD model, where the surfaces subjected to least-squares fitting operations are highlighted (A, P, C) (a); different section planes based on conventional alignment and on the improved alignment for one of the seven reference levels (b).

The axis of the fitting cylinder is intersected with the horizontal fitting plane to obtain a point. By repeating this routine for all the reference fiducials, a total of 21 points are obtained. More specifically, these points are three per plane, hence defining a total of 7 planes at different heights along the building direction. As explained in Section 2.1, the planes are used to gather information on possible deviations and deformations of the part on different height levels. Figure 3b represents an example of a local reference level (coloured in blue) which is determined following this approach.

As it comes to post-process analyses, it is common practice to extract CT cross-sections parallel to a reference plane as the one shown in red in Figure 3b and described as “conventional (global) alignment”, whose normal represents the building direction. The extracted cross-section can then be compared to images gathered during the LPBF process monitoring using an on-machine sensing technique. Despite this strategy is the simplest that can be applied, it is based on the simplified hypothesis that no part distortions arise after the fabrication. However, the iterative nature of LPBF results in a sequence of heating and cooling cycles, typically leading to shrinkage and deformation phenomena. Figure 4a demonstrates that these deformations are not negligible. In fact, the CT cross-section obtained through the global alignment (i.e. red plane in Figure 3b) is far different from the corresponding nominal section. On the contrary, the CT cross-section obtained by using the nearest local alignment reference plane (i.e. blue plane in Figure 3b) is much closer to the nominal.

What has been discussed is particularly critical for in-process monitoring, where the layer data are actually acquired on a plane parallel to the platform (hence close to the nominal layer position) and stacked vertically by a spacing equal to the nominal layer thickness. In order to effectively use CT to compare the anomalies detected during the process with actual after-build defects and validate process monitoring methods, the data alignment accuracy is fundamental to reducing the amount of false positives and false negatives.

The actual need to employ an alignment that considers local deformations was confirmed by the results obtained in this research.

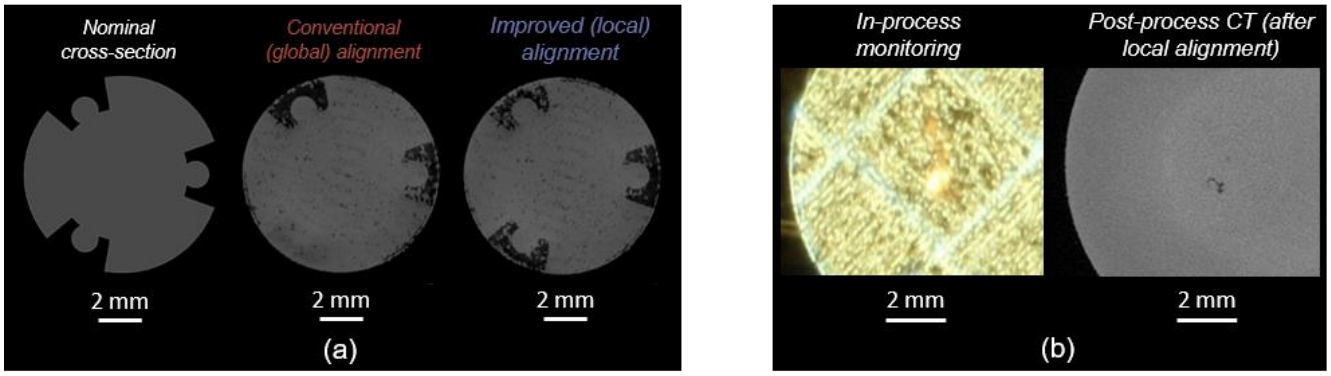

Figure 4 – Comparison of CT cross-sections obtained via conventional global and newly proposed local alignment. The nominal section is reported on the left as a reference (a); comparison of a process signature and the corresponding CT cross-section, extracted by following the local alignment (b).

4 Comparison of in-process LPBF monitoring data and post-process CT data

The developed alignment method has been applied in the correlation of LPBF process signatures with actual defects detected in the post-process through CT. The in-process monitoring system used was composed by a high-resolution Digital Single Lens Reflex (DSLR) camera installed with off-axis positioning with respect to the building direction. An image per layer was acquired with the long-exposure technique, where the resulting image is a consequence of the integration of the emitted radiation generated from the interaction between the laser beam and the powder bed.

An example of obtained image is reported in Figure 4b (left), where a hot spot due to a spatter particle (i.e. particles that are ejected from the zone of interaction between the laser and the powder bed) is visible. The corresponding CT cross-section extracted by means of the local alignment proposed in this work is also represented in Figure 4b (right). It shows a defect in the same location where the spatter was found. The defect was instead not detected using the conventional alignment. Such defect is a pore surrounding a circular solid particle, which is typical of lack-of-fusion porosities caused by spatters. The proposed alignment method enabled the accurate comparison of in-process LPBF monitoring data with post-process CT measurements, with two important outcomes: (i) the detected hot spot was identified as a relevant process anomaly leading to an actual defect within the fabricated part, and (ii) the hot spot was determined to be caused by a spatter particle causing a localized lack-of-fusion region. Results like these are fundamental to lay the foundations for improving the understanding of LPBF process dynamics and moving forward an automatic and active process control.

5 Conclusions and future work

This paper elaborated on the first results of a research work that is focused on the alignment of in-process additive manufacturing monitoring data and post-process CT measurements, whose accuracy is fundamental to achieve a robust comparison and to unlock a wider understanding of metal LPBF processes. The work is based on the design of a sample characterized by a number of reference fiducials, which allow taking into account in the alignment the tridimensional deformations occurring after the fabrication. Both additive manufacturing and metrology-related guidelines were applied in the design phase. Alongside this, an alignment procedure developed based on the designed geometry was also discussed. The methodology was then applied to actual samples fabricated by LPBF of Ti6Al4V and compared with the traditional alignment approach, which is instead done by considering the building direction and the nominal layer thickness, and simplistically assuming that no relevant deformations occur between the monitoring period and the post-process quality control.

Such traditional approach has proven to be not suited for experiments striving for accurately correlating process signatures with actual flaws. On the contrary, CT cross-sections extracted by means of the proposed local alignment have shown to be much more accurate when compared to the corresponding nominal sections. The importance of a robust alignment was further demonstrated by applying the method to a case study where process signatures related to spatter particles were detected and correlated to actual lack-of-fusion porosities, which are only present in the CT cross-sections obtained through the improved alignment.

Future work will be focused on quantifying the deviations between the two alignments and investigating other geometries.

References

[1] Gibson I., Rosen D., Stucker B., Khorasani M. (2021). Additive manufacturing technologies. New York: Springer.

[2] Naghshineh B., Carvalho H. (2022). The implications of additive manufacturing technology adoption for supply chain resilience: A systematic search and review. International Journal of Production Economics 247. https://doi.org/10.1016/j.ijpe.2021.108387.

[3] Warnke P.H., Douglas T., Wollny P., Sherry E., Steiner M., Galonska S., Becker S. T., Springer I. N., Wiltfang J., Sivananthan S. (2009). Rapid Prototyping: Porous Titanium Alloy Scaffolds Produced by Selective Laser Melting for Bone Tissue Engineering. Tissue Engineering Part C: Methods, 15:115-124, https://doi.org/0.1089=ten.tec.2008.0288.

[4] Everton S. K., Hirsch M., Stravroulakis P., Leach R. K., Clare A.T. (2016). Review of in-situ process monitoring and in-situ metrology for metal additive manufacturing. Materials & Design 95:431:445. https://doi.org/10.1016/j.matdes.2016.01.099.

[5] Spears T.G., Gold S.A. (2016). In-Process Sensing in Selective Laser Melting (SLM) Additive Manufacturing. Integrating Materials and Manufacturing Innovation 5, 1:25. https://doi.org/10.1186/s40192-016-0045-4

[6] Mani M., Feng S., Lane B., Donmez A., Moylan S., Fesperman R. (2015). Measurement science needs for real-time control of additive manufacturing powder bed fusion processes. NISTIR 8036. http://dx.doi.org/10.6028/NIST.IR.8036

[7] Craeghs T., Bechmann F., Berumen S., Kruth J. P. (2010). Feedback control of layerwise laser melting using optical sensors. Physics Procedia 5:505–514. https://doi.org/10.1016/j.phpro.2010.08.078.

[8] Grasso M., Remani A., Dickins A., Colosimo B. M. (2021). In-situ measurement and monitoring methods for metal powder bed fusion – an updated review. Meas. Science and Technology 32. https://doi.org/10.1088/1361-6501/ac0b6b.

[9] Lane B., Moylan S., Whitenton E., Ma L. (2016). Thermographic measurements of the commercial laser powder bed fusion process at NIST. Rapid Prototyping Journal, 22:778–787. https://doi.org/10.1108/RPJ-11-2015-0161.

[10] Goossens L., Van Hooreweder B. (2021). A virtual sensing approach for monitoring melt-pool dimensions using high speed coaxial imaging during laser powder bed fusion of metals. Additive Manufacturing 40. https://doi.org/10.1016/j.addma.2021.101923.

[11] Imani F., Gaikwad A., Montazeri M. (2018). Process mapping and in-process monitoring of porosity in laser powder bed fusion using layerwise optical imaging. Journal of Manufacturing Science and Engineering 140. https://doi.org/10.1115/1.4040615.

[12] Aminzadeh M., Kurfess T. (2016). In-situ quality inspection of laser powder bed fusion using high-resolution visual camera images. Solid Freeform Fabrication.

[13] Caltanissetta F., Grasso M., Petrò S., Colosimo B.M. (2018). Characterization of in-situ measurements based on layerwise imaging in laser powder bed fusion. Additive Manufacturing 24:183:199. https://doi.org/10.1016/j.addma.2018.09.017.

[14] Mc Cann R., Obeidi M. A., Hughes C., McCarthy E., Egan D. S., Vijayaraghavan R. K., Joshi A. M., Acinas Garzon V. Dowling P. D., McNally P. J., Brabazon D. (2021). In-situ sensing, process monitoring and machine control in Laser Powder Bed Fusion: A review. Additive Manufacturing 45. https://doi.org/10.1016/j.addma.2021.102058.

[15] Leach R., Carmignato S., eds (2020), Precision Metal Additive Manufacturing. CRC Press, Boca Raton.

[16] Benedetti M., Fontanari V., Bandini M., Zanini F., Carmignato S. (2018). Low- and high-cycle fatigue resistance of Ti-6Al-4V ELI additively manufactured via selective laser melting: Mean stress and defect sensitivity. International Journal of Fatigue 107:96-109, https://doi.org/10.1016/j.ijfatigue.2017.10.021.

[17] Lu Q. Y., Nguyen N. V., Hum A. J. W., Tran T., Wong C. H. (2020). Identification and evaluation of defects in selective laser melted 316L stainless steel parts via in-situ monitoring and micro computed tomography. Additive Manufacturing 35. https://doi.org/10.1016/j.addma.2020.101287.

[18] Ferrucci M., Craeghs T., Cornelissen S., Pavan M., Dewulf W., Donmez A. (2021). Lessons learned in the design of reference fiducials for layer-wise analysis of test coupons made by laser powder bed fusion. Additive Manufacturing 42. https://doi.org/10.1016/j.addma.2021.101997.

[19] Coeck S., Bisht M. (2019). Prediction of lack of fusion porosity in selective laser melting based on melt pool monitoring data. Additive Manufacturing 25:347-356. https://doi.org/10.1016/j.addma.2018.11.015.

[20] Bonato N., Zanini F., Bernardi L., Carmignato S. (2022). On the alignment of in-process and post-process measurement datasets acquired for precision enhancement of laser powder bed fusion of metals. Euspen 22nd International Conference and Exhibition, Geneva, CH.

[21] Hermanek P., Carmignato S. (2016). Reference object for evaluating the accuracy of porosity measurements by X-ray computed tomography. Case Studies in Nondestructive Testing and Evaluation 6:122-127. https://doi.org/10.1016/j.csndt.2016.05.003.